VOLUME 10 NUMBER 2 FEBRUARY 2007
www.nature.com/natureneuroscience

nature neuroscience

Hippocampal place cells in bats

Notch regulates olfactory neuron identity

Altruism and detection of agency

nature neuroscience

Hippocampal cellular and network activity in freely moving echolocating bats

Nachum Ulanovsky[1,2] & Cynthia F Moss[1–3]

The hippocampus is crucial for episodic and spatial memory. In freely moving rodents, hippocampal pyramidal neurons show spatially selective firing when the animal passes through a neuron's 'place-field', and theta-band oscillation is continuously present during locomotion. Here we report the first hippocampal recordings from echolocating bats, mammals phylogenetically distant from rodents, which showed place cells very similar to those of rodents. High-frequency 'ripple' oscillations were also rodent-like. Theta oscillation, however, differed from rodents in two important ways: (i) theta occurred when bats explored the environment without locomoting, using distal sensing through echolocation, and (ii) theta was not continuous, but occurred in short intermittent bouts. The intermittence of theta suggests that models of hippocampal function that rely on continuous theta may not apply to bats. Our data support the hypothesis that theta oscillation in the mammalian hippocampus is involved in sequence learning and hence, theta power should increase with sensory-input rate—which explains why theta power correlates with running speed in rodents and with echolocation call rate in bats.

In vivo recordings from the rodent hippocampus have revealed several characteristic activity patterns at the cellular and network levels that have been central to theories of hippocampal function: place cells, high-frequency ripple oscillations and theta oscillation are among the most widely studied. Place cells are pyramidal neurons whose activity increases when the animal passes through a restricted area of the environment, the place field, and are thought to be important for navigation[1–3]. Ripples are brief high-frequency oscillations (120–200 Hz) observed during slow-wave sleep that are thought to be involved in transferring stored information to the neocortex during memory consolidation[4–9]. Theta oscillation is a slow (5–10 Hz) oscillation that occurs continuously for many minutes during exploration, locomotion and rapid eye movement (REM) sleep[6,10,11], and it has been central to numerous computational models of hippocampal function (reviewed in ref. 12).

Are these hippocampal activity patterns universal across all mammalian species? In primates, data from hippocampal recordings seem to present a somewhat different picture than is seen in rodents. Although place cells have been reported in monkeys[13,14], some studies found neurons that were sensitive to where the monkey was directing its gaze and proposed that this 'spatial-view tuning' can explain the place tuning of monkey hippocampal neurons[15]; both place cells and spatial-view cells have been reported in the human hippocampus[16]. Ripples were recorded in human hippocampus[17] and appear to be similar to those observed in rodents. Continuous or nearly-continuous hippocampal theta has been found in several mammalian species during locomotion, including rabbits, dogs and cats[18] (and also in homing pigeons[19]); however, theta oscillation has not been consistently recorded in primate hippocampus[18] and those studies that reported theta in primates described several differences from rodents. First, in both monkeys[20] and humans[21] theta has low amplitude and is mixed with large, low-frequency delta waves. Second, hippocampal theta in primates is not continuous, as it is in rodents, but occurs in short bouts in monkeys under urethane anesthesia[20], humans performing a virtual navigation task[21] and humans during REM sleep[22] (but see ref. 23, which reported a continuous delta-band oscillation with some theta-like characteristics in human hippocampus during REM sleep.) Theta-bout durations of 1–2 s were reported in primates[21,22], and in behaving humans theta was present during $<10\%$ of total session time[21]. This intermittent nature of theta in primates has potentially important implications for computational models of hippocampal function, many of which posit a continuous theta oscillation.

Reported differences in hippocampal activity among animals may be due to differences in behavior between species. Alternatively, they may be due to methodological issues: for example, the geometry of the primate hippocampus, especially its thick pyramidal layer[24], may not favor optimal summation of dipoles to generate large field potentials in the theta range; brain activity differences may also be due to differences in behavioral tasks, or in recording methods, such as electrode impedances or placements. Here, we studied hippocampal activity *in vivo* in echolocating bats, a model animal that allowed us to test these two possibilities.

Echolocating bats are nocturnal mammals, phylogenetically distant from rodents[25], which produce short ultrasonic calls and use the returning echoes to orient and forage for fruits, insects and even vertebrates, such as frogs and fish[26,27]. Bats have excellent spatial

[1]Department of Psychology, [2]Institute for Systems Research, [3]Neuroscience and Cognitive Science Program, University of Maryland, College Park, Maryland 20742, USA. Correspondence should be addressed to N.U. (nulanovsky@psyc.umd.edu).

Received 18 July 2006; accepted 12 December 2006; published online 7 January 2007; doi:10.1038/nn1829

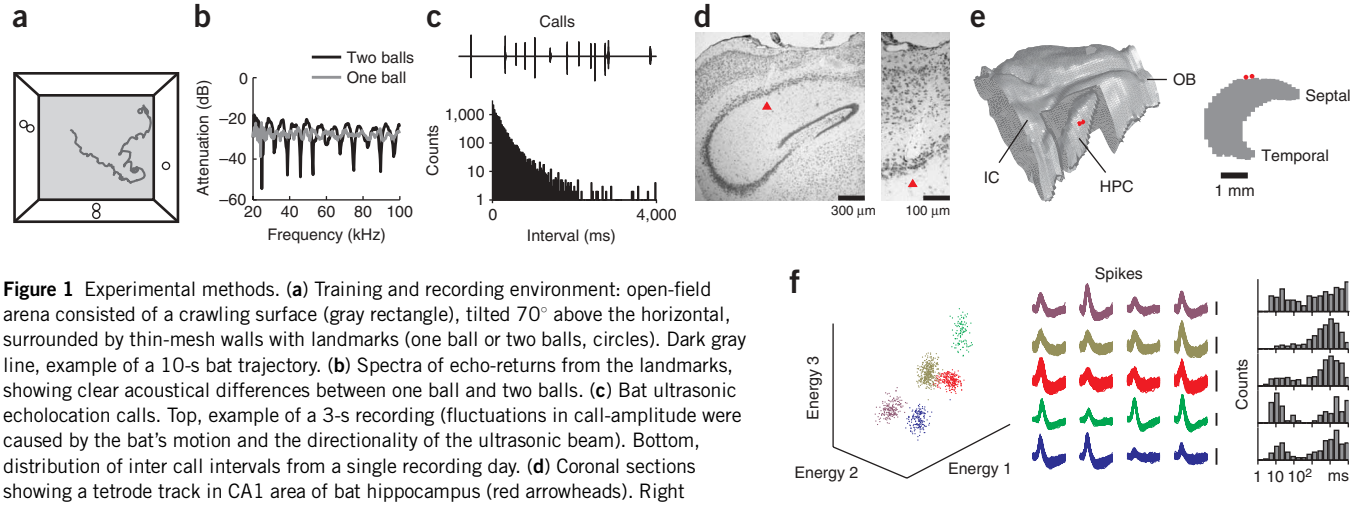

Figure 1 Experimental methods. (**a**) Training and recording environment: open-field arena consisted of a crawling surface (gray rectangle), tilted 70° above the horizontal, surrounded by thin-mesh walls with landmarks (one ball or two balls, circles). Dark gray line, example of a 10-s bat trajectory. (**b**) Spectra of echo-returns from the landmarks, showing clear acoustical differences between one ball and two balls. (**c**) Bat ultrasonic echolocation calls. Top, example of a 3-s recording (fluctuations in call-amplitude were caused by the bat's motion and the directionality of the ultrasonic beam). Bottom, distribution of inter call intervals from a single recording day. (**d**) Coronal sections showing a tetrode track in CA1 area of bat hippocampus (red arrowheads). Right picture, at higher magnification, is one section posterior to left picture. (**e**) Locations of tetrode penetrations (red dots) on a three-dimensional reconstruction of the bat's brain (left) and on a side-view of the hippocampus (right). Left, OB, olfactory bulbs; IC, inferior colliculus; HPC, hippocampus, revealed by digitally removing a 'window' of overlying cortex. Total anterior-posterior length shown, 7.7 mm. Right, lateral view of the hippocampus alone (dorsal is upward, anterior is to the right). Tetrode tracks were much closer to the septal pole of the hippocampus than to its temporal pole. (**f**) Spike sorting (cluster cutting) of spikes recorded on one tetrode. Data are from all five sessions of one day. Left, 'cluster plot', three-dimensional plot showing energy of spikes (dots) on three of the tetrode's channels; five single units are seen (five clusters, colored separately). Middle, 'waveform plot', spike waveforms from the five units (rows) on all four tetrode channels (columns), with colors corresponding to the clusters on the left; all the raw waveforms, from all five sessions, are shown superimposed. Vertical scale bars, 200 μV; waveform duration, 1 ms; negativity is up. Right, 'interval histograms', distributions of interspike intervals for these five pyramidal cells (logarithmic time scale, from 1 ms to 100 s; ticks on abscissa denote 1, 10, 10^2, 10^3, 10^4 and 10^5 ms).

memory on many spatial scales: from long-distance migration and homing in some species[28], through the use of reproducible 'flyways' between roosting and foraging sites[29], to their remarkable ability to find particular spots inside a cave on the centimeter scale[30]. Although bats typically forage aerially, it has been shown that when crawling, bats use absolute space–based (allocentric) navigation[31]—a navigational strategy that in rodents is hippocampus dependent[1]. Notably, as we show here, bats present two advantages as model animals for hippocampal studies. First, they use two distinct behavioral modes of spatial exploration, as primates do, which readily allows the comparison of behavioral correlates of theta oscillations between bats, rodents and primates. Secondly, it proved possible to adopt for bats methodologies that are used in rodents: tetrode recordings from hippocampal area CA1 of freely foraging animals. Together with the rodent-like thin pyramidal layer of bats, this allowed us to address the methodological issues that have constrained comparative interpretations of rodent and primate data.

Here we conducted the first hippocampal recordings from freely moving echolocating bats. Our recordings showed well-defined place cells and ripples, which were very similar to those in rodents. Unlike in rodents, however, theta oscillation occurred in short, intermittent bouts lasting 1–2 s. Moreover, the theta bouts occurred when the bats explored the environment by echolocating and without locomoting—quite the opposite from the behavioral contingency of theta oscillation in rodents.

RESULTS

We trained two big brown bats (*Eptesicus fuscus*; weight, 15–18 g) to crawl and forage in an open-field arena for randomly placed tethered mealworms ('mealworm-chasing' task; **Fig. 1a**). Polystyrene balls, hanging singly or in pairs on the arena walls (**Fig. 1a**, circles), served as proximal landmarks, both for the visual modality and for echolocation (**Fig. 1b**). Recording days consisted of five 20-min sessions: three sleep sessions and two behavioral sessions, an 'echolocation-only' session in complete darkness and 'echolocation + vision' session with lights available. These behavioral sessions allowed us to test the stability of place fields across different sensory conditions. During both behavioral sessions the bats produced echolocation calls with highly irregular intercall intervals (**Fig. 1c**); average intervals were similar between the two sessions (mean interval: 236 and 237 ms, respectively; median: 161 and 141 ms) and also similar to the average intercall intervals used during flight in the so-called 'search mode'[32]. Under both light and dark conditions, bats continuously produced echolocation calls[26] and stopped echolocating only when chewing mealworms (and during sleep sessions).

After the bats were trained in the foraging task, they were implanted with a miniature tetrode microdrive and tetrodes were advanced toward dorsal hippocampal area CA1 (**Fig. 1d,e**). After the bats recovered from surgery, we recorded daily from them as they performed the foraging task. The positions of two light-emitting diodes on the bat's head were tracked and field potentials and spiking activity were recorded from the CA1 pyramidal layer. The spike waveforms were later spike-sorted to isolate single units (**Fig. 1f**), totaling 154 pyramidal cells from two bats.

Hippocampal place cells

We found spatially selective place cells in the bat hippocampus. Fewer than half of the pyramidal cells recorded were active during either of the behavioral sessions (64/154 cells, 42%); the other cells stopped firing during both behavioral sessions and resumed firing during sleep (**Fig. 2a**), similar to the 'silent cells' reported in rodents[33]. We computed a firing-rate map for each active cell by partitioning the arena into bins and dividing the number of spikes by the time the bat spent in each bin (**Fig. 2b**). Some active cells had diffuse spatial firing (17/64, 27%; see Methods), but the majority of active cells had spatially restricted place fields and were termed 'place cells' (47/64, 73%;

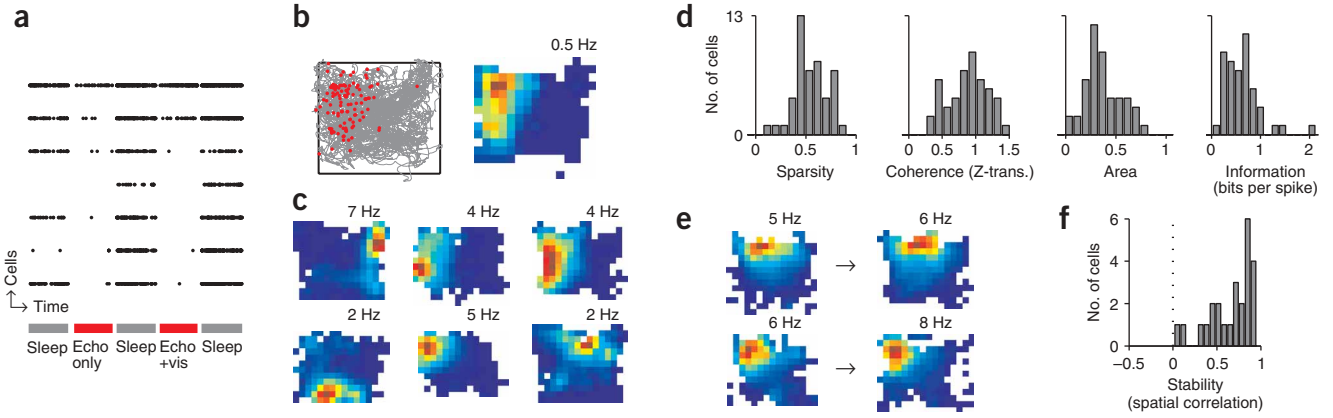

Figure 2 Place cells in bat hippocampal area CA1. (**a**) Activity patterns of seven pyramidal cells recorded simultaneously on one tetrode, showing occurrences of spikes (dots) during sleep sessions (gray bars) and the absence of spiking in most cells during the two behavioral sessions (red bars; 'echolocation-only' and 'echolocation + vision' sessions). Each session lasted 20 min; spikes recorded between sessions were excluded. (**b**) Computing the firing-rate map of one pyramidal cell. Left, trajectory of bat (gray) with superimposed spikes (red); rectangle, edges of crawling-surface. Right, color-coded firing-rate map; color scale is linear, with blue corresponding to zero and red to peak firing rate (indicated on top) and white color indicating bins where the bat spent <1 s. Data are from 'echolocation + vision' session. (**c**) Firing-rate maps of six additional cells (two from 'echolocation-only' sessions, four from 'echolocation + vision' sessions). Peak firing rate (corresponding to red color) is indicated above each cell. (**d**) Population histograms of four indices quantifying the spatial selectivity of place cells ($n = 47$ cells): sparsity, spatial coherence (*Z*-transformed), place-field area (above 20% of maximal rate) and spatial information. (**e**) Firing-rate maps of two cells (the two rows), showing stability of place fields across the two behavioral sessions (columns). (**f**) Population histogram of the spatial correlation (two-dimensional correlation) between firing-rate maps in the two behavioral sessions ($n = 25$ cells; see Methods). The high correlation values (median, $r = 0.74$) demonstrate that most place fields were stable across sessions.

Fig. 2c). The percentage of place cells out of the total population of well-isolated pyramidal neurons (47/154, 31%) was very similar to the percentage reported for rats (ref. 3: 98/288 cells, 34%).

To quantify the spatial selectivity of the place cells, we computed four commonly used indices—sparsity, coherence, spatial information and area of place field (see Methods)—and constructed population histograms (**Fig. 2d**). These indices showed a range of values that was fairly similar to that seen in the same indices reported for rat dorsal CA1 cells in an open-field arena[34,35]. Because our recordings were slightly further from the septal pole of the hippocampus than typical dorsal CA1 recordings in rats (**Fig. 1d**,**e**) and place fields in rats are narrowest near the septal pole of the hippocampus[36,37], it is likely that, in the bat, place cells located more septally would have even tighter place fields than are shown here.

We next examined the stability of place fields between the echolocation-only and echolocation + vision sessions (**Fig. 2e**). We selected those cells that showed stable firing rates across all three sleep sessions (25/47, 53%; see Methods) and computed the spatial correlation between place fields in the two behavioral sessions. Most cells showed correlations >0.74, indicating stable place fields (**Fig. 2f**). This distribution of spatial correlations was very similar to that reported for rat CA1 (ref. 35). Moreover, whereas spatial correlations in rats have been computed between two identical conditions (re-run in same environment), here we used the same environment but allowed the use of different available sensory modalities. Therefore, these results suggest that place fields in bats are as stable as those in rats.

High-frequency ripple oscillations

During sleep, short bouts of high-frequency ripple oscillations occurred in the local field potential (LFP) recorded from the CA1 pyramidal layer and were accompanied by an increase in the firing rate of cells (**Fig. 3a**). Spectral analysis of the LFP revealed a peak between 80–160 Hz (**Fig. 3b**). The population average frequency of the peak's maximum was 123.4 ± 1.2 Hz (mean ± s.e.m.), which is lower in frequency than the 140–200-Hz ripples of rats[5] or the 120–180-Hz ripples of the mouse[6], but higher than the ~100-Hz ripples observed in humans[17].

As in rodents, ripples had their maximum amplitude in the pyramidal layer (**Fig. 3c**). The ripples occurred at irregular times, but often occurred as 'ripple doublets', manifested by a ~100-ms peak in the inter-ripple interval histogram (**Fig. 3d**). This histogram was very similar to data reported for the mouse[6]. The duration of ripples was 48.6 ± 23.8 ms (mean ± s.d.), which is similar to that observed in rodents[5,6].

To examine the temporal relationships between ripples and single-cell firing, we aligned individual ripples on their trough and plotted the population average ripple (**Fig. 3e**) and the ripple-triggered firing rate averaged over all cells, on the same time axis (**Fig. 3f**). The firing rate showed a marked increase concurrent with the ripples. On average, cells increased their firing rate >10 times compared to baseline (**Fig. 3f**, right inset). Furthermore, spikes were phase-locked to the ripple oscillations on a millisecond timescale, with the maximal firing rate occurring during the trough of the ripples (**Fig. 3f**, left inset). This phase relationship is the same as that observed in the rat[5] and mouse[6]. Taken together, our data indicate that ripples in bats seem to have very similar properties to ripples in rodents.

Hippocampal theta oscillation

To study theta oscillation, we first characterized the bat's spatial behaviors. This was necessary because previous studies suggest that theta is behavior dependent in all species; for example, in freely running rats theta occurs during exploration and locomotion and is absent during immobility[10,18,38], whereas in cats, theta is maximal in immobile animals that are engaged in active visual searching, visual fixation or tracking of prey[18,38], although theta is also observed during locomotion[18].

Echolocating bats can explore the environment by locomoting, or by scanning the environment using echolocation, or both. Therefore, to

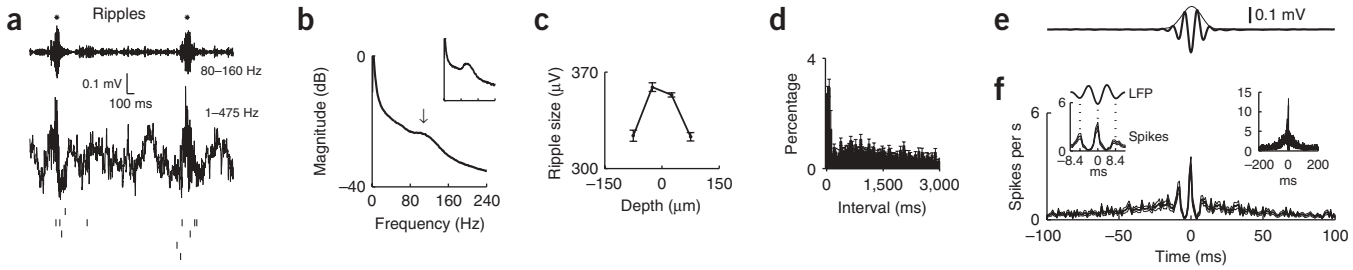

Figure 3 High-frequency ripple oscillations in bat hippocampus. (**a**) Example of local field potential (LFP) recording, showing two ripples (asterisks). Top LFP trace, filtered (80–160 Hz); middle LFP trace, unfiltered (1–475 Hz); positivity is up. Bottom, spikes of five pyramidal cells (vertical ticks) that discharged simultaneously with the ripples. (**b**) Spectral power of LFP (log scale) during sleep in a single recording day (data from all three sleep sessions). Note peak between 80–160 Hz (arrow). Inset, spectral power of data taken from 1-s segments around each ripple; same axes as in main plot. (**c**) Depth profile of ripple amplitude (peak to peak) from one bat. Error bars are mean ± s.e.m. Shown is nominal depth, with 0 corresponding to the average depth over all recordings sites (approximately center of CA1 pyramidal layer). (**d**) Distribution of inter-ripple time intervals, averaged over all recording days for both bats ($n = 27$ days). Error bars are mean ± s.e.m. (**e**) Average ripple waveform (thick line) with ripple power (thin line). Same timescale as in **f**. This average waveform was computed using the filtered LFP (80–160 Hz). (**f**) Ripple-triggered firing rate, averaged over all cells (thin lines, mean ± s.e.m.; $n = 154$ cells). Left inset, blow-up in time of the firing rate ('spikes') and the average ripple waveform ('LFP'), showing the phase-locking of cells; dotted lines at –8.4, 0 and +8.4 ms mark the ripple oscillation troughs. Right inset, firing rate normalized by the baseline rate (mean rate between –500 and +500 ms around each ripple).

characterize the bat's behavior, we computed its velocity of motion and its echolocation call rate and plotted them together, revealing two behavioral modes (**Fig. 4a**): (i) Mode 1, or 'exploration without locomotion', when the bat was nearly stationary (low velocity), and explored the environment using relatively high call rates, and (ii) Mode 2, or 'exploration by locomotion', when the bat was locomoting, and used lower call rates. Spatial maps of the occurrences of these modes indicated that both modes occurred almost everywhere in the arena (**Supplementary Fig. 1** online).

To analyze theta separately for these two behavioral modes, we delineated mode 1 (**Fig. 4b**, blue) and the high-velocity portion of mode 2 (red), as well as the low velocity/low-call-rate data (black). We then extracted the appropriate time epochs and plotted the LFP power spectrum separately for each (**Fig. 4c**,**d**). Most recording sites showed a clear theta peak between ~5–7 Hz, but only during behavioral mode 1 (**Fig. 4c**, blue). This was also evident in the population average (**Fig. 4d**, blue). The occurrence of theta during mode 1 was also supported by histograms of the theta-to-delta ratio[5,6], which is a commonly used index of theta occurrence (defined as theta-band LFP power, between 4 and 8 Hz, divided by delta-band power, between 2 and 4 Hz; see **Supplementary Fig. 2** online). Thus, bat hippocampus showed theta oscillation during mode 1 but not during mode 2, akin to what occurs in cats but unlike in rodents.

The small theta peak (**Fig. 4d**) was similar to the small theta peak reported from monkey[20] and human[21] hippocampi and quite different from the large, prominent theta peak in rodents[10]. Two different explanations (or a combination of both) for a small spectral peak in the theta range are that theta oscillation is continuous, but has small peak-to-peak voltage, or that theta has large voltage, but is intermittent, occurring in short, discrete bouts. Our data indicated that theta oscillation in the bat occurs in short, large-amplitude bouts, suggesting that the second possibility was correct. This is shown in an example of a 7-Hz theta bout during behavior (**Fig. 5a–e**) and an example from sleep (**Fig. 5f**). The theta bouts could be observed both in the LFP voltage traces (**Fig. 5a**,**c**) and in spectrogram displays (frequency × time, **Fig. 5d**). Large, low-frequency delta waves often occurred before and after the theta bout (**Fig. 5c**, black trace), which is similar to that seen in monkeys[20]. To extract the theta episodes from the commonly occurring background of delta waves, we used the theta-to-delta ratio. This ratio had a low average value, 0.603 ± 0.737 (population mean ± s.d.), interspersed with short bouts of high values that accompanied the bouts of theta oscillation in the LFP (**Fig. 5a–c**). Using a theta-to-delta ratio of 2.0 as a threshold (**Supplementary Fig. 2**), we extracted above-threshold 'theta bouts' versus below-threshold 'non-theta epochs' (all of the results below were qualitatively similar when other threshold values were used). Theta bouts occurred approximately twice a minute

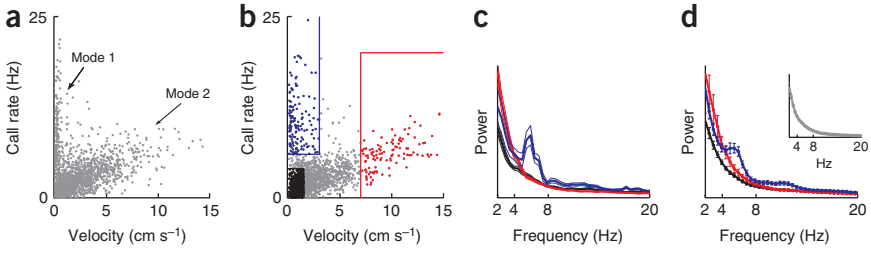

Figure 4 Behavior-dependent theta oscillation in the hippocampus of echolocating bats. (**a**) Rate of echolocation calls versus locomotion velocity, computed in 2-s windows with 1-s overlap (dots), showing exploratory modes 1 and 2. Data are from one recording day, pooled over both behavioral sessions. In mode 2, the call rate was positively correlated with velocity (median correlation over all recording days, excluding mode 1 data, $r = 0.668$). For display purposes, dots were jittered in the *y*-direction, to compensate for the call rate discretization due to counting in a finite window (jitter size, 0.5 Hz = 1 divided by the 2-s window-size). (**b**) Example from another recording day, with colors denoting mode 1 (blue dots), the high-velocity portion of mode 2 (red dots) and low velocity–low call rate (black dots). The borders used for defining these three 'behavioral areas' (colored lines) were the same for all recording days: velocity ≤ 3 cm s^{-1}, call rate ≥ 6 Hz (blue); velocity ≥ 7 cm s^{-1}, call rate ≤ 20 Hz (red); velocity ≤ 1.5 cm s^{-1}, call rate ≤ 4 Hz (black). (**c**) Spectral power of LFP (linear scale) from one recording day, computed separately for each 'behavioral area' in **b** (colors as in **b**). Thin lines are mean ± s.e.m. (**d**) Population average spectral power of LFP, computed by averaging single-day power spectra over all recording days from both bats; error bars are mean ± s.e.m. ($n = 27$ d). Main plot, behavioral sessions (colors as in **b**). Inset, sleep sessions.

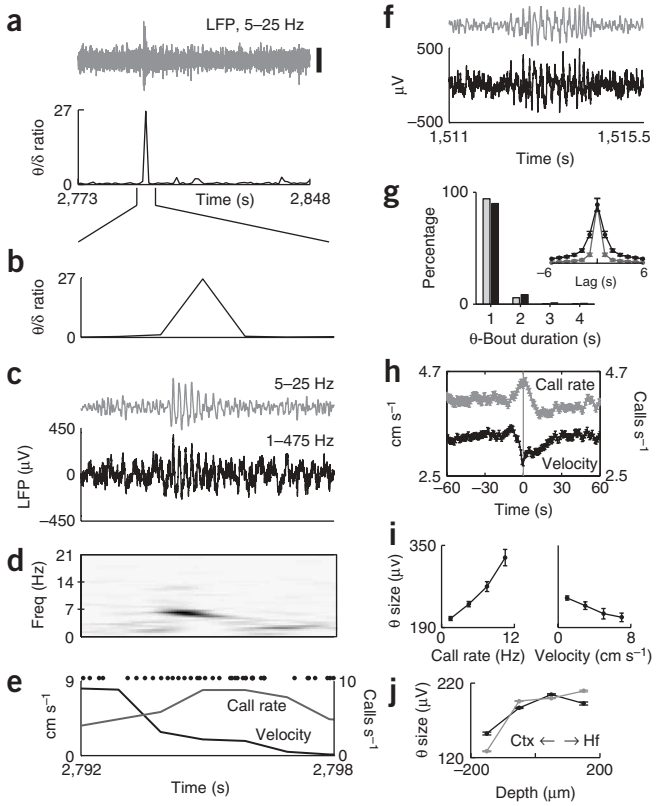

Figure 5 Properties of theta oscillation in bat hippocampus. (**a**) Example of filtered LFP (top) and theta-to-delta ratio (bottom) versus time, during behavior, showing a clear theta bout. Segment duration is 75 s; scale bar on top is 200 μV. (**b**–**e**) Blow-up in time of a 6-s segment around the theta bout seen in **a**; panels **b**–**e** share a common time axis. (**b**) Theta-to-delta ratio. (**c**) LFP traces. Black, unfiltered, 1–475 Hz; gray, filtered between 5–25 Hz; positivity is up. (**d**) Spectrogram (frequency × time) of the LFP, computed using a 2,048-point fast Fourier transform with 97% overlap. Linear color scale, white denotes low power and black high power. (**e**) Call rate and locomotion velocity (line plots). Dots are times of individual calls. (**f**) Example of a theta bout during sleep; same filtering as in **c**. (**g**) Theta bouts have durations of 1–2 s. Main plot, distribution of theta-bout durations during behavior (black) and sleep sessions (light gray). Inset, autocorrelograms of the theta-to-delta ratio (dark gray) and of the LFP voltage (filtered in the theta band, black), during behavior. Autocorrelograms were computed separately for each recording day and averaged across days and the average was normalized by its maximum (error bars are mean ± s.e.m., $n = 27$ d). (**h**) Theta bout–triggered average call rate (gray) and average velocity (black), demonstrating that around the center time of a theta bout (time 0) there was an increase in call rate and a decrease in velocity. The error bars denote population mean ± s.e.m. The two *y*-axes have the same numerical ranges for the velocity and call rate. (**i**) Peak-to-peak voltage of theta bouts versus call rate (left) and versus velocity (right); error bars are population mean ± s.e.m. (**j**) Depth profile of theta voltage during behavior (black) and sleep sessions (gray). Data are from both bats; error bars are mean ± s.e.m.; depth of 0 μm corresponds to the nominal center of CA1 pyramidal layer. Theta oscillation had its minimal size above the pyramidal layer, toward the cortex (Ctx) and increased in size below the pyramidal layer, toward the hippocampal fissure (Hf).

(average inter-bout interval, computed using intervals of <300 s, was: behavior, 33.4 ± 35.1 s; sleep, 25.5 ± 27.6 s; mean ± s.d.). The duration of bouts was typically 1–2 s (**Fig. 5g**), which is similar to theta-bout durations reported from human hippocampus[21,22]. This duration of 1–2 s was measured in three ways: (i) directly from the time extent that the theta-to-delta ratio was above threshold (**Fig. 5g**, main plot), (ii) from the autocorrelogram of the theta-to-delta ratio (**Fig. 5g** inset, dark gray), which had an autocorrelation length of ~1–2 s, and (iii) from the autocorrelogram of the peak-to-peak voltage of the LFP (where the LFP was filtered in the theta range, 4–8 Hz; **Fig. 5g** inset, black), which also had an autocorrelation length of ~1–2 s.

The theta bout example in **Fig. 5c** was accompanied by an increased call rate and a decreased locomotion velocity (**Fig. 5e**), precisely the behavioral contingency in which the LFP spectrum showed a theta peak (**Fig. 4c–d**, blue). This contingency was further supported by two population analyses. First, theta bout–triggered average call rate and average velocity curves (**Fig. 5h**) showed that around the center time of a theta bout (time 0) there was an increase in call rate and a decrease in locomotion velocity. Note that call rates did not go down to zero outside of the theta bouts, reflecting the fact that the bats never stopped vocalizing; moreover, their call rates of several calls per second also meant that multiple calls occurred within a single, 1–2 s theta bout (for example, **Fig. 5e**, dots). Second, we filtered the LFP in the theta range (4–8 Hz) and plotted the peak-to-peak voltage during theta bouts versus the call rate (**Fig. 5i**, left) and versus the velocity (**Fig. 5i**, right), showing that theta voltage increased with call rate and decreased with velocity (one-way ANOVA: call rate, $F_{3,2577} = 42.24$, $P < 10^{-32}$; velocity, $F_{3,2576} = 6.71$, $P < 0.0002$; *t*-test of the theta voltage between the two extreme groups: call-rate, $t = 10.73$, degrees of freedom (d.f.) = 1,338, $P < 10^{-25}$; velocity, $t = 3.94$, d.f. = 1,739, $P < 10^{-4}$). These results are consistent with the behavioral contingency for theta seen in the previous analyses (**Fig. 4**) and suggest that theta bouts indeed corresponded to behavioral mode 1. Note that this contingency is the opposite of that observed in rats, where theta increases with velocity[37].

Depth profiles of theta amplitude demonstrated that theta voltage increased as the tetrode was moved in depth from above the CA1 pyramidal layer to below it, toward the hippocampal fissure (**Fig. 5j**), during both behavior (black) and sleep (gray) (*t*-test of theta voltage in the two extreme depth bins: behavior, $P < 10^{-46}$; sleep, $P < 10^{-99}$). This depth profile was qualitatively similar to depth profiles of theta in rodents, where theta amplitude also increases in size toward the hippocampal fissure[6,11]. We also plotted depth profiles of the percentage of time occupied by theta bouts, but these did not reveal any correlation with depth (**Supplementary Fig. 3** online; all four correlation coefficients, for two bats × sleep versus behavior, $P > 0.05$). This lack of correlation is incongruous with the idea that theta bouts reflect amplitude fluctuations of a continuous theta oscillation because in that case we would expect a large increase in the percentage of time occupied by theta bouts as the tetrode is lowered toward the hippocampal fissure—which was not the case—but it is congruous with theta bouts being actual discrete events. Furthermore, analysis of theta size showed that, for the highest call rate group, the average voltage was >320 μV (**Fig. 5i**, left) and in many cases the voltage of theta bouts approached half a millivolt (for example, **Fig. 5c**,**f**)—a large-sized oscillation, which is inconsistent with the notion of a small theta that barely rises above the noise, but is consistent with the notion of discrete high-amplitude theta bouts.

We also observed theta bouts during sleep (**Fig. 5f**) but there was no theta spectral peak during sleep (**Fig. 4d**, inset). This absence of a theta peak was probably caused by the low percentage time of theta bout occurrence during sleep (**Supplementary Fig. 3**) and by the fact that the LFP spectrum was computed over the entire sleep session.

Finally, we asked whether the firing of neurons was related to the theta oscillation. Average firing rates were slightly lower during

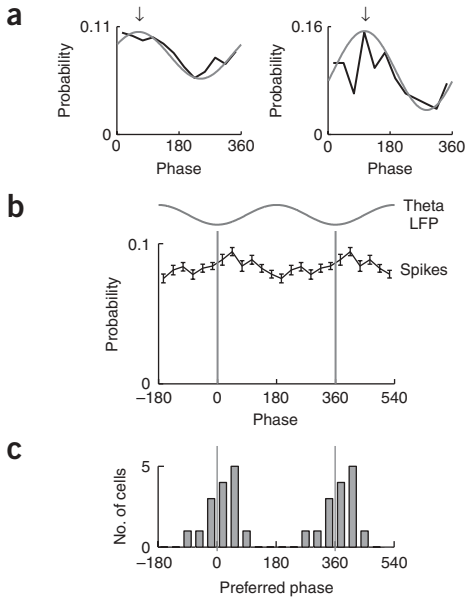

Figure 6 Theta phase modulation of pyramidal cell firing. (**a**) Examples of phase distributions of the discharges of two neurons (black), together with the best-fitting cosine functions (gray). Data from theta bouts in all five sessions were pooled together. Arrows show the preferred theta phase of the two cells (defined as the location of the cosine's peak). (**b**) Black curve, population average discharge probability, computed over all the neurons that fired five or more spikes per phase-bin on average[5] ($n = 35$ cells); error bars are mean ± s.e.m. Gray curve, average field theta wave (filtered between 4–8 Hz). Two theta cycles are shown for visualization purposes. (**c**) Distribution of preferred phases for those neurons that had a significant cosine fit (that is, significant correlation between the cell's phase distribution and the best-fitting cosine; $n = 15$ cells). The most common preferred phase occurred slightly after the trough of the locally-recorded theta wave (phase 0).

behavioral mode 1, when theta was present, compared with mode 2 (mean ± s.d. of the firing rate: 0.95 ± 0.57 compared with 1.24 ± 0.63 Hz, respectively, computed for cells with a total of >1,000 spikes from both behavioral sessions; *t*-test, $P < 0.005$), which is similar to that observed in the mouse, where the firing rates of pyramidal neurons are lower during theta than during non-theta behaviors[6]. The firing rates during theta bouts did not show a significant dependence on either call rate or locomotion velocity (one-way ANOVA of firing rates, using the same call-rate and velocity groups as in **Fig. 5i**: call rate, $F_{3,112} = 1.80$, $P > 0.15$; velocity, $F_{3,112} = 0.60$, $P > 0.5$). Next, we analyzed the relation between neural firing and theta phase. We filtered the LFP in a narrow frequency band (4–8 Hz) at the theta range and used the cycle-by-cycle troughs of the theta oscillation to compute the theta phase that corresponded to each spike of every neuron (**Fig. 6**). In many neurons, the spike discharges showed clear phase-locking to the theta oscillation (**Fig. 6a**, black curves), which was well fitted by a cosine function (gray). This theta modulation of firing rates was also seen at the population average phase distribution (**Fig. 6b**). We also computed the preferred phase for each neuron (the phase of the best fitting cosine function; for example, **Fig. 6a**, arrows) and plotted the histogram of preferred phases for those neurons where the cosine-fit was significant (**Fig. 6c**). This histogram showed a very clear theta modulation. In fact, the general form of the histogram (**Fig. 6c**) and the numerical value of the most common preferred phase (which was slightly after the trough of the locally recorded theta oscillation) were remarkably similar to the same histograms reported for CA1 pyramidal neurons in rodents[5,6].

DISCUSSION

Here we reported on the first study of hippocampal activity *in vivo* in echolocating bats, which have two distinct exploratory modes. This allows for a direct comparison with hippocampal data from rodents and primates, which opens the door to a broad across-species understanding of hippocampal function. We focused on three neural activity patterns: place cells, high-frequency ripple oscillations and theta oscillation. First, most of the active neurons (47/64, 73%) were place cells with spatially selective and stable place fields, similar to those seen in rodents (**Fig. 2**). Second, high-frequency ripple oscillations were associated with a phase-locked firing of cells at the same phase as is seen in rodents (**Fig. 3**). Finally, theta oscillation with a 5–7 Hz frequency was observed (**Figs. 4** and **5c**,**d**). As is seen in rodents, the amplitude of theta increased toward the hippocampal fissure (**Fig. 5j**) and neurons' discharges were phase-locked to the theta oscillation with the same phase as in rodents (**Fig. 6**). Theta oscillation in bats, however, also differed from theta in rodents in three ways. First, the theta spectral peak was small and was accompanied by a large delta-band component. Second, theta was not continuous as it is in freely running rodents, but occurred in short bouts with durations of 1–2 s. Third, and most important, theta had a very different behavioral contingency than has been observed in rodents: the theta bouts occurred during a behavioral mode (mode 1, **Fig. 4**) in which bats used echolocation to explore the environment from a fixed location, without locomoting.

These results corroborate findings of intermittent theta from monkeys[20] and humans[21,22]. The validity of previous reports on intermittent theta in primates may be questioned, however, on several grounds. First, the pyramidal layer in primates is much thicker than in rodents[24], potentially leading to nonoptimal summation of theta-generating dipoles, which may explain why theta recorded from the human hippocampus has an extremely small voltage, 30–40 μV peak to peak[21], which is 1–2 orders of magnitude smaller than in rats[18,37]. Second, there were several methodological differences between experiments in primates and in rodents, which may have affected the LFP recordings. These include the electrodes used in monkeys[20] and humans[21], which differed from the tetrodes typically used in rodents[3,39], and differences in the behavioral tasks or in the subject's ability to locomote freely. In our experiments, however, we used tetrodes with properties identical to those of the tetrodes used in rodents and a behavioral task that was analogous to a task widely used in rodents[2]. Moreover, the big brown bats that we studied have a thin CA1 pyramidal layer (**Fig. 1d**), like rodents, and in addition, the theta oscillation that we found in the bats had a maximal amplitude of ~0.5 mV (**Fig. 5c**,**f**), which is much larger than in humans[21] and is quite similar to the theta amplitude recorded in CA1 pyramidal layer of rats[5,37] and mice[6]. Thus, we conclude that the differences we observed between bats and rodents, including the intermittent nature of theta in bats and its different behavioral contingency, are indeed real differences.

Our results have some interesting implications for models of mammalian hippocampal function. For example, because many such models rely on continuous theta oscillation[12], our finding of intermittent bouts of theta—bouts that occur on average only twice a minute—raises questions about the general applicability of these models to all mammals. Thus, models of oscillatory encoding and retrieval of memories via the theta cycle[40] may not be suitable for bats, as it seems unlikely that memories are encoded and retrieved only twice a minute. Similarly, theta in bats probably occurs too rarely to be involved in navigational mechanisms, as bats can locomote substantial

distances between the theta bouts, although experimental findings on the 'theta phase precession' of neural firing[34,39,41], as well as certain models[12], have implicated theta in rodent navigation. On the other hand, our results provide support for other theories of hippocampal function. In particular, the finding of place cells in the bat hippocampus supports the notion that hippocampal pyramidal neurons are involved in spatial processing.

Our finding of differences in brain activity between bats and rodents adds to a list of brain areas where interspecies differences in neural activity have been reported, including differences in network oscillations (**Supplementary Discussion**). Evolutionary history may explain some interspecies differences and similarities in brain activity, but it does not seem to provide a consistent picture in the case of hippocampal theta (see ref. 25 and **Supplementary Discussion**). It is more likely, therefore, that interspecies differences in the theta rhythm are driven by differences in how the animals use their sensory systems to explore the environment. Rats and mice have poor vision and mainly use proximal senses (olfactory and somatosensory), which require that they explore space by locomotion. In contrast, primates, cats and bats have good distal senses (vision in primates and cats, echolocation in bats), which they can use to explore space without locomoting. These behavioral differences may be reflected by differences in theta oscillation[38].

What are the common behavioral principles that may underlie the reported interspecies differences in theta? Two hypotheses come to mind. First, hippocampal theta oscillation has been subdivided into type 1 'atropine-resistant' theta, present during locomotion, and type 2 'atropine-sensitive' theta, present during immobility in rabbits (and under some conditions also in rats) in response to sensory stimuli[18,42]. Type 2 theta has been suggested to be involved in sensory processing relevant to the initiation and maintenance of voluntary motor behaviors[42]. In bats, one may hypothesize that the theta bouts observed during high call rates were type 2 theta and that they were involved in maintaining the motor patterns of echolocation, which are known to be influenced by sensory inputs[27]. This hypothesis can be viewed as being in broad agreement with the sensorimotor integration theory of theta[42]. It does not, however, explain the absence of type 1 theta during locomotion in bats.

A second hypothesis involves the notion that theta is important in the processing of stimuli across time and in learning of temporal sequences[34,43,44]. Thus, we hypothesize that maximal theta may be expected when sensory information arrives at high rates or changes rapidly. In rats, which rely mostly on proximal senses, new olfactory and somatosensory information arrives most rapidly when the animal runs at high velocities, and hence we would expect theta amplitude to increase with running velocity, as is indeed the case[37]. In bats, which rely on echolocation, the rate of sensory input is controlled by the animal itself, via changes in the echolocation call rate. Therefore, we would expect theta amplitude to increase with the call rate, as we found here (**Fig. 5i**).

Similar hypotheses can be suggested for primates, which lead to the prediction that in behaving primates, theta oscillation might be related to active visual exploration by eye movements. Individual saccades have indeed been shown to modulate the firing rate of monkey hippocampal neurons[45]. Furthermore, a saccade can be thought of as a discrete species-specific unit of information intake[45], similar to an echolocation call in the bat and an olfactory sniff in the rat. Notably, theta oscillation seems to be phase-locked to the sniffing cycle during high sniffing rates in the rat[46], and theta is maximal during high call rates in the bat. Therefore, we hypothesize that characterization of the behavioral exploratory modes of the monkey, using locomotion velocity and rate of saccades as the two behavioral parameters (similarly to our **Fig. 4**), would reveal theta bouts that are mostly occurring during high rate of saccades, that is when the animal is exploring the environment by making several saccades per second.

Finally, the differences that we found in the properties of theta oscillation may be due to the crawling of our bats. Thus, it is possible that, during flight, continuous theta oscillation would be observed in the bat hippocampus and that in rapidly flying bats the amplitude of theta oscillation would be positively correlated with flight speed. Nevertheless, our results provide a positive example of a behavior, foraging by crawling in an open-field arena, during which place fields were present, concurrently with intermittent bouts of theta.

In summary, our results underscore the need to conduct further comparative studies of hippocampal function; for example, it would be interesting to determine whether spatial-view cells similar to those reported in monkeys[15] exist in bat hippocampus, and whether the activity of such spatial-view cells, or of place cells, is modulated by the bat's spatial-exploration mode (mode 1 versus mode 2). Such a comparative and ethological approach[47] could help reveal the properties of hippocampal function that are invariant across species, and these invariances may be important for a deeper understanding of the function of mammalian hippocampus.

METHODS

Subjects. Two adult big brown bats were studied in these experiments, using procedures approved by the University of Maryland Animal Care and Use Committee. The bats were collected from the attics of private homes in Maryland and housed in a vivarium, where they were kept on a 12-h reversed light-dark cycle and were allowed free access to water. Bats were fed mealworms (*Tenebrio molitor*) and food supplements and throughout the training and recording period were maintained at approximately 90% of their *ad libitum* weight (18 and 15 g for the two bats, respectively).

Training and recording environment. The training and recording environment was a 68 × 73 cm rectangular arena, composed of a nylon-mesh floor, on which the bats crawled, surrounded by walls made of mist nets (40 cm high; mist nets were made of very fine threads with 25-mm spacing). The floor and walls were attached to a rigid plastic frame (**Fig. 1a**). The arena floor, walls and frame were all colored black. The arena was tilted so that its floor was 70° above the horizontal (almost vertical); this arrangement was chosen because bats generally prefer to crawl on vertical or nearly vertical surfaces. Polystyrene balls (3.8 cm in diameter) served as proximal landmarks and were hung either singly or in pairs on the arena walls in an asymmetric (polarized) arrangement that was fixed throughout the training and recording periods (**Fig. 1a**, circles); either white or dark balls were used, depending on the behavioral session. The arena was positioned on the floor of a large room (7.2 × 6.4 × 2.5 m) that was lined with sound-absorbing foam (Sonex-1, Acoustical Solutions) to reduce echo reverberations. A few pieces of electronic equipment were placed against the walls of the room and served as distal landmarks (because the arena had no ceiling, several such landmarks, which were located directly in front of the tilted arena, were unobstructed by its walls). The positions of the distal landmarks were fixed during a recording day and across most days, but some of the distal landmarks were moved between recording days.

Echo-return measurements. We performed echo-return measurements, which showed that the acoustic return spectra of the proximal landmarks (one ball versus two balls) were very distinct (**Fig. 1b**). The series of notches in the two-ball spectrum is caused by interference of echoes returning from the two balls, so-called two-wavefront interference, with the frequency intervals between notches being inversely proportional to the difference in the distance from the bat to the two balls (**Fig. 1b**, the two-ball spectrum was measured for a 2.7-cm difference). These bats can easily discriminate between such spectra[48]. Because this difference in distance depends on the cosine of the angle from the bat to the line connecting the balls, which in turn depends on the bat's location in the arena, these landmarks provided an acoustic positional cue for the bat.

Echo-return measurements were taken by playing wideband sound pulses (10–110 kHz downward frequency-modulated chirps) via an amplifier (S55, Ultrasound Advice) and a custom-made ultrasonic speaker and recording the echoes using a microphone with an amplifier (UM3, Ultrasound Advice) followed by a filter (Wavetek model 852). These measurements also showed that the echo power from the highly reflective balls was >15 dB stronger than the echoes from the fine-threaded arena walls (data not shown), so the bat could readily detect the balls on the background of the walls.

Behavioral training. The bat's task was to crawl freely on the tilted 'floor' of the arena (**Fig. 1a**, gray rectangle), termed the crawling surface, in order to find a ~100-mg mealworm that was threaded at the end of a monofilament line (0.1 mm in diameter) and was hung 1–2 cm from the crawling surface. The mealworms were placed at random locations in the arena, and were sometimes jittered or moved slightly to attract the attention of the bat. The bats eventually learned to crawl vigorously in search of the mealworms. This foraging task in an open-field arena is similar to the 'pellet chasing' task commonly used in hippocampal studies of rats[2] and hence was termed a 'mealworm chasing' task.

During pretraining, the bats were introduced into the arena, which was placed against the room wall, and were presented with threaded mealworms. Initially, the bats spent most of their time hanging head-down at the top of the crawling surface, exploring the arena using echolocation without locomoting, and sometimes tried to fly away. When the bats reached a good level of performance (that is, when they easily found every mealworm, crawled through every part of the arena numerous times during each session and did not fly away), the arena was moved to its final position in the middle of the room and the bats were trained daily for the same duration of time as during the subsequent recordings.

At the start and end of each recording day the arena was thoroughly cleaned with alcohol, to remove odors. Each recording day consisted of five sessions (20 min each): three sleep sessions (sessions no. 1, 3 and 5) interspersed with two behavioral sessions. The behavioral sessions differed by the available sensory information. One session was an 'echolocation-only' session, in which all lights were turned off and the experimenter was wearing night-vision goggles (NVG7-2+, ATN Corp.) and the second was an 'echolocation + vision' session, in which lights were available (sessions no. 2 and no. 4, respectively). (The original reason for using these two behavioral sessions was to test certain theories on 'spatial-view cells'[15], but these analyzes will not be presented in this paper; here we compared data from the two sessions only when analyzing place-field stability, see **Fig. 2e**,**f**.) We used dark-colored polystyrene balls during the echolocation-only session, whereas during the echolocation + vision session these balls were replaced with high-contrast white balls, with identical sizes and locations as the dark ones. During sleep sessions the bat slept on a cloth at the bottom of a ceramic pot, adjacent to the arena.

Light-level measurements. Light measurements were done using a sensitive illuminance meter (IL-1700, International Light). During the echolocation-only behavioral session all lights were turned off, resulting in illuminance levels $<10^{-5}$ lx, well below the vision threshold of this bat species[49] (or of humans). The light-emitting diodes used for tracking the bat's position increased the illumination at the arena to between $< 10^{-4}$ lx and 0.13 lx (the light levels varied depending on the viewing direction; 0.13 lx was measured when the illuminance meter was pointing directly head-on at the light-emitting diodes), but the dark-colored landmarks remained virtually invisible to the human eye, even after dark adaptation. During the echolocation + vision behavioral session, the room was illuminated with a daylight–spectrum lamp (SoLux, Tailored Lighting), which produced a dim illumination at the arena that varied in the range of 0.2–6.0 lx, well within the 1–10 lx range that is optimal for vision in this bat species[49].

Surgery and recording. After learning the task, these small bats (weight 15–18 gr) were chronically implanted with a four-tetrode microdrive, which was originally developed for the mouse (4-drive, Neuralynx). Tetrodes[3,39] (~45-μm diameter) were constructed from four strands of polyimide-coated Ni-Cr wire (Rediohm-800, 12.7 μm in diameter, Kanthal Palm Coast), bound together by twisting and then melting their insulation. Four tetrodes were loaded and glued into a nested assembly of polyimide tubes and mounted into the lightweight 2.1-g microdrive. The tetrodes exited the microdrive through a guide cannula in an approximately rectangular arrangement with ~600-μm horizontal spacing and every tetrode could be moved independently via a drive screw (160 μm per turn). Each tetrode was cut flat and its tip was gold-plated to reduce the impedance of individual wires to 0.5–1.0 MΩ (at 1 kHz). While the bat was under isoflurane anesthesia, the skull was micro-scarred to improve subsequent adhesion and a square opening (approximately 1.4 × 1.4 mm) was made in the skull over the right hemisphere, above the dorsal hippocampus. The center of the craniotomy was 1.8 mm lateral to the midline and 2.6 mm anterior to lambda (*Big Brown Bat Stereotaxic Brain Atlas*, E. Covey, University of Washington, in preparation). After the removal of the dura, the tip of the microdrive's guide tube was placed on the brain surface and the craniotomy was filled with a biocompatible elastomer (Kwik-Sil, World Precision Instruments) to protect the brain. The exposed muscle tissues were covered with a thin layer of biocompatible adhesive (Vetbond, World Precision Instruments) for protection and the skull and microdrive's base were then covered with cyanoacrylate adhesive (Loctite 4013, Henkel).

During a period of ~1 week after surgery, the tetrodes were slowly lowered toward the CA1 pyramidal layer. One of the tetrodes served as a reference and was left in an electrically-quiet zone (bat 1: at brain surface, above the hippocampus; bat 2: in white matter, medially to the lateral ventricle). This reference tetrode was used for differential recordings. The remaining three tetrodes served as recording probes, although in each bat we were able to obtain high-quality recordings only from one recording tetrode. The positioning of the tetrodes in the CA1 pyramidal layer was provisionally determined by the presence of high-frequency field oscillations (ripples) and associated neuronal firing and was later verified histologically.

During recordings, a unity-gain preamplifier (HS-16, Neuralynx) was attached to a connector on top of the microdrive and connected via a lightweight tether to a commutator (PSR-24, Neuralynx) mounted in the ceiling of the recording room; the tether was also connected to a counter-weight system, to reduce the load on the bat's head. Signals from each of the tetrode's four wires were amplified (×2,000) and band-pass filtered (600–6,000 Hz, Lynx-8, Neuralynx) and a voltage threshold (typically 55–80 μV) was used for collecting 1-ms spike waveforms, which were sampled at 32 kHz (0.25 ms before the peak and 0.75 ms after, Cheetah data acquisition system, Neuralynx). One of the tetrode's wires was also used for collecting continuous recordings of the local field potential, or LFP (×1,000 gain, 1–475 Hz filtering, 2-kHz sampling rate). Tetrodes were moved between recording days upward or downward, as necessary, to maximize the quality of spike data recorded in each day.

A video tracker (Neuralynx) was used to track the positions of two light-emitting diodes located at the top of the preamplifier. The *x*, *y* positions of the diodes were sampled at a rate of 30 Hz and the center point between the two diodes was taken as the head's position.

The timing of the bat's echolocation calls was recorded by filtering a 31–39-kHz frequency slab, around the peak spectral energy of the bat's ultrasonic calls, and heterodyning it down in frequency to 0–8 kHz using a bat detector (D-230, Pettersson Elektronik) and then sampling it continuously at 16 kHz (Cheetah data acquisition system, Neuralynx). The heterodyning distorted the spectral structure of the echolocation calls, but permitted an accurate measurement of call timing.

All types of data (spikes, LFP, video, audio) were timestamped with the same 1-MHz clock (Cheetah Digital I/O, Neuralynx). Data were collected continuously throughout the five sessions of each recording day (~2 h daily).

Spike sorting. Spike waveforms that occurred simultaneously (within <0.5 ms) on all of the recording tetrodes were discarded as artifacts. The waveforms were then separated on the basis of their relative energies on different channels of each tetrode. We used a graphical-clustering method ('cluster cutting'[3,34]), whereby each spike was plotted as a dot in a three-dimensional graph representing the energy of the spike on three of the tetrode's four channels (**Fig. 1f**, left), using software that allowed three-dimensional rotations and translations of these data (SpikeSort3D, Neuralynx). Data from all five sessions were spike sorted together. Well-isolated clusters of spikes were manually encircled with polygons and were color coded. To verify the correspondence of these clusters to well-isolated single units, we checked that a refractory period (2 ms) was present in the interspike interval histogram (**Fig. 1f**, right) and the amplitudes of all the waveforms from each cluster were

well above the voltage threshold of the data-acquisition system (that is, the voltage threshold was not cutting a low-amplitude cluster in the middle). This allowed us to isolate up to 16 simultaneously recorded cells from a single tetrode (5.7 cells per tetrode, on average).

Putative pyramidal (complex-spike) cells were identified according to the following four criteria: (i) the spike waveform had a characteristic shape with a narrow peak followed by a long afterhyperpolarization trough (**Fig. 1f**, middle), (ii) the average firing rate, over all the sessions, was <5 Hz (**Supplementary Fig. 4** online), (iii) interspike interval histograms had a bimodal shape, with the lower peak at $\sim$10 ms, indicating the presence of complex-spike bursts (**Fig. 1f**, right), and (iv) the cell was recorded simultaneously with other complex-spike cells (in the CA1 pyramidal layer). We were not able to isolate single-unit interneurons, possibly because we used a rather high voltage threshold (typically 55–80 μV).

We analyzed here only well-isolated pyramidal neurons that discharged $\geq$100 spikes over all five sessions. This yielded a total of 154 well-isolated pyramidal neurons from 27 recording days in 2 bats. Of these pyramidal cells, we termed as 'active cells' those neurons that discharged $\geq$40 spikes in at least one of the two behavioral sessions (64/154 cells, or 42%; on average we had 2.4 active cells per tetrode). The other cells were termed 'silent cells' (90/154, 58%): these neurons discharged $\geq$40 spikes per session only during sleep sessions[33] (**Fig. 2a**).

Data analysis. For extracting high-frequency ripples, the LFP recording was digitally band-pass filtered between 80–160 Hz (see **Fig. 3a**). The power (absolute value of the Hilbert transform) of the band-pass–filtered LFP signal was computed and the threshold for ripple detection was set to 7 s.d. above the mean power[5]. The duration of ripples was computed based on the portion of the signal above the 7-s.d. threshold. For calculating the ripple-triggered average firing rate of single units (**Fig. 3f**), the troughs of the ripples (filtered between 80–160 Hz) were used as the reference point (time 0).

For extracting theta epochs, we calculated the ratio of the power in the theta (4–8 Hz) and delta (2–4 Hz) frequency bands, in 2-s windows. A theta-to-delta ratio of 2.0 was used as our threshold criterion (other thresholds yielded similar qualitative results). Power spectra were computed using Welch's method and a Hamming window with 2,048 samples and 50% overlap (for computing the spectra of theta we digitally downsampled the LFP signal to 1 kHz, whereas for computing the spectra of ripples we used the original 2-kHz sampling rate). Behavioral parameters (bat's velocity and echolocation call rate, **Fig. 4a**,**b**) were computed in the same 2-s windows as the power spectra and the theta-to-delta ratio. Because the bat's velocity and call-rate parameters were similar in the two behavioral sessions, data from both behavioral sessions were pooled together when analyzing theta oscillations. Those 2-s windows in which motion artifacts were present, as judged by the LFP power increasing $>$10 times above the mean power, were discarded from the analyses.

Because we did not conduct sleep-staging measurements and because the very short durations of the theta bouts precluded LFP-based sleep staging, we pooled together the data from the entire sleep session when analyzing sleep recordings, both for the analysis of ripples and for the analysis of theta occurrence during sleep. This pooling may have contributed to the small size of the ripples power spectrum (**Fig. 3b**) and to the lack of theta spectral peak during sleep (**Fig. 4d**, inset).

Firing-rate maps for single units were computed by partitioning the arena into 5 $\times$ 5 cm bins and dividing the number of spikes that occurred within each bin by the time spent by the bat within that bin. Bins in which the bat spent $<$1 s during the session were excluded from the firing-rate map and were colored white (**Fig. 2b**,**c**,**e**). For display purposes only, the maps were smoothed with a 3 $\times$ 3–bin triangular window.

To quantify the spatial selectivity of the cells, we used four indices: spatial coherence, area of place field, spatial information per spike and sparsity. Spatial coherence[2,35] is the correlation between the firing rates in the original firing map and the firing rates averaged across the eight neighbors of each bin. The coherence was computed from nonsmoothed maps and was Fisher Z-transformed to facilitate comparisons with previous studies[35]. Cells with Z-transformed coherence $<$ 0.4 (17/64 of the active cells, 27%) were considered as having spatially diffuse firing and were not included in the population analysis (**Fig. 2d**); the nondiffuse cells (47/64, 73%) were considered place cells. Area of place field was defined as the proportion of bins with a firing rate $\geq$20% of the maximum firing rate, but only including bins for which at least two of the eight neighbors also had a firing rate $\geq$20% of the maximum. Spatial information per spike[34,50] (bits per spike) is equal to $\sum p_i(r_i/r)\log_2(r_i/r)$, where r_i is the firing rate of the cell in the i^{th} bin of the place-field, p_i is the probability of the bat being in the i^{th} bin (time spent in the i^{th} bin/total session time), $r = \sum p_i r_i$ is the overall mean firing rate and i is running over all the bins where the bat spent $\geq$1 s. Sparsity[34] is equal to $\langle r_i\rangle^2/\langle r_i^2\rangle = (\sum p_i r_i)^2/\sum p_i r_i^2$. The sparsity and area indices are bound between 0 and 1 and the spatial information is a positive number, whereas the Z-transformed spatial coherence can have either negative or positive values. For the sparsity and area indices, low values indicate good spatial selectivity, and for the coherence and information indices, high values indicate good spatial selectivity. For the population histograms (**Fig. 2d**), we averaged for each place cell the indices computed for the two behavioral sessions (consequently, the counts shown in these histograms reflect the true number of cells, as we did not double count cells across the two behavioral sessions).

For computing the stability of the place fields across the two behavioral sessions, we used only cells that were well-isolated throughout the five sessions and that were stably active during all three sleep sessions ($\geq$40 spikes per session in each sleep session; 25 cells). For each cell, the place-field stability was quantified by computing the spatial correlation (two-dimensional correlation coefficient) between the place fields in the two behavioral sessions.

For all statistical tests in this study we used a $P < 0.05$ significance level.

Histology. After the completion of the experiments, the bats were given an overdose of sodium pentobarbital (120 mg per kg of body weight) and, with the tetrodes left *in situ*, were perfused transcardially using 50 ml of saline followed by 50 ml of fixative (4% paraformaldehyde, 0.1 M phosphate buffer). The brain was removed and a block around the hippocampus was cut and placed in fixative for 72 h at 4 °C, embedded in paraffin and coronal sections (10 μm) were cut with a microtome. The sections were Nissl-stained with cresyl violet and tetrode placements in the CA1 pyramidal layer were verified using a light microscope fitted with a digital camera.

For the three-dimensional reconstruction of the bat's brain (**Fig. 1e**), we measured the brain outline and hippocampus outline from the stereotaxic brain atlas of the big brown bat (E. Covey). Measurement of hippocampus outline was circumscribed by the CA1 and CA3 pyramidal layers and the dentate granule cell layer.

Note: Supplementary information is available on the Nature Neuroscience website.

ACKNOWLEDGMENTS

We thank K.D. Harris, M. Lengyel, A. Sirota, J. Siegel, S. Cowan, M. Aytekin, K. Ghose and J. Fritz for critically reading the manuscript, G. Sutherland and B. McNaughton for invaluable technical advice during N.U.'s visit to the Arizona Research Laboratories, J. Lisman, N. Kopell, A.D. Redish, W. Hodos, G. Wilkinson, K. Macleod, S. Sinha, C. Stengel, R. Harlan, T. Barnes and A. Graybiel for helpful discussions and technical advice, B. Falk for help with experiments, E. Covey for a preprint of the bat brain atlas, E. Sanovich for histology and C. Carr for use of the Neurolucida system. This research was supported by US National Institutes of Health grant R01 MH56366 to C.F.M. and by the Center for Neuroscience at the University of Maryland.

AUTHOR CONTRIBUTIONS

N.U. designed the study, conducted the experiments, analyzed the data and wrote the manuscript. C.F.M. supervised the project.

COMPETING INTERESTS STATEMENT

The authors declare that they have no competing financial interests.

Published online at http://www.nature.com/natureneuroscience
Reprints and permissions information is available online at http://npg.nature.com/reprintsandpermissions

1. O'Keefe, J. & Nadel, L. *The Hippocampus as a Cognitive Map* (Oxford University Press, Oxford, 1978).
2. Muller, R.U., Kubie, J.L. & Ranck, J.B., Jr. Spatial firing patterns of hippocampal complex-spike cells in a fixed environment. *J. Neurosci.* **7**, 1935–1950 (1987).
3. Wilson, M.A. & McNaughton, B.L. Dynamics of the hippocampal ensemble code for space. *Science* **261**, 1055–1058 (1993).

4. Buzsáki, G., Horváth, Z., Urioste, R., Hetke, J. & Wise, K. High-frequency network oscillation in the hippocampus. *Science* **256**, 1025–1027 (1992).
5. Csicsvari, J., Hirase, H., Czurkó, A., Mamiya, A. & Buzsáki, G. Oscillatory coupling of hippocampal pyramidal cells and interneurons in the behaving rat. *J. Neurosci.* **19**, 274–287 (1999).
6. Buzsáki, G. *et al.* Hippocampal network patterns of activity in the mouse. *Neuroscience* **116**, 201–211 (2003).
7. Siapas, A.G. & Wilson, M.A. Coordinated interactions between hippocampal ripples and cortical spindles during slow-wave sleep. *Neuron* **21**, 1123–1128 (1998).
8. Kudrimoti, H.S., Barnes, C.A. & McNaughton, B.L. Reactivation of hippocampal cell assemblies: effects of behavioral state, experience, and EEG dynamics. *J. Neurosci.* **19**, 4090–4101 (1999).
9. Sirota, A., Csicsvari, J., Buhl, D. & Buzsáki, G. Communication between neocortex and hippocampus during sleep in rodents. *Proc. Natl. Acad. Sci. USA* **100**, 2065–2069 (2003).
10. Vanderwolf, C.H. Hippocampal electrical activity and voluntary movement in the rat. *Electroencephalogr. Clin. Neurophysiol.* **26**, 407–418 (1969).
11. Buzsáki, G. Theta oscillations in the hippocampus. *Neuron* **33**, 325–340 (2002).
12. Lengyel, M., Huhn, Z. & Érdi, P. Computational theories on the function of theta oscillations. *Biol. Cybern.* **92**, 393–408 (2005).
13. Ono, T., Nakamura, K., Nishijo, H. & Eifuku, S. Monkey hippocampal neurons related to spatial and nonspatial functions. *J. Neurophysiol.* **70**, 1516–1529 (1993).
14. Ludvig, N., Tang, H.M., Gohil, B.C. & Botero, J.M. Detecting location-specific neuronal firing rate increases in the hippocampus of freely-moving monkeys. *Brain Res.* **1014**, 97–109 (2004).
15. Georges-François, P., Rolls, E.T. & Robertson, R.G. Spatial view cells in the primate hippocampus: allocentric view not head direction or eye position or place. *Cereb. Cortex* **9**, 197–212 (1999).
16. Ekstrom, A.D. *et al.* Cellular networks underlying human spatial navigation. *Nature* **425**, 184–188 (2003).
17. Bragin, A., Engel, J., Jr., Wilson, C.L., Fried, I. & Buzsáki, G. High-frequency oscillations in human brain. *Hippocampus* **9**, 137–142 (1999).
18. Robinson, T.E. Hippocampal rhythmic slow activity (RSA; theta): a critical analysis of selected studies and discussion of possible species-differences. *Brain Res.* **203**, 69–101 (1980).
19. Siegel, J.J., Nitz, D. & Bingman, V.P. Hippocampal theta rhythm in awake, freely moving homing pigeons. *Hippocampus* **10**, 627–631 (2000).
20. Stewart, M. & Fox, S.E. Hippocampal theta activity in monkeys. *Brain Res.* **538**, 59–63 (1991).
21. Ekstrom, A.D. *et al.* Human hippocampal theta activity during virtual navigation. *Hippocampus* **15**, 881–889 (2005).
22. Cantero, J.L. *et al.* Sleep-dependent theta oscillations in the human hippocampus and neocortex. *J. Neurosci.* **23**, 10897–10903 (2003).
23. Bódizs, R. *et al.* Rhythmic hippocampal slow oscillation characterizes REM sleep in humans. *Hippocampus* **11**, 747–753 (2001).
24. Amaral, D.G. & Lavenex, P. Hippocampal neuroanatomy. in *The Hippocampus Book* (eds. Andersen, P., Morris, R.G., Amaral, D.G., Bliss, T.V. & O'Keefe, J.) 37–114 (Oxford University Press, New York, 2007).
25. Springer, M.S., Stanhope, M.J., Madsen, O. & de Jong, W.W. Molecules consolidate the placental mammal tree. *Trends Ecol. Evol.* **19**, 430–438 (2004).
26. Griffin, D.R. *Listening in the Dark* (Yale University Press, New Haven, 1958).
27. Schnitzler, H.-U., Moss, C.F. & Denzinger, A. From spatial orientation to food acquisition in echolocating bats. *Trends Ecol. Evol.* **18**, 386–394 (2003).
28. Griffin, D.R. Migration and homing of bats. in *Biology of Bats* Vol. 1 (ed. Wimsatt, W.A.) 233–264 (Academic Press, New York, 1970).
29. Williams, T.C. & Williams, J.M. Radio tracking of homing and feeding flights of a neotropical bat, *Phyllostomus hastatus*. *Anim. Behav.* **18**, 302–309 (1970).
30. McCracken, G.F. Locational memory and female-pup reunions in Mexican free-tailed bat maternity colonies. *Anim. Behav.* **45**, 811–813 (1993).
31. Mueller, H.C. & Mueller, N.S. Sensory basis for spatial memory in bats. *J. Mamm.* **60**, 198–201 (1979).
32. Surlykke, A. & Moss, C.F. Echolocation behavior of big brown bats, *Eptesicus fuscus*, in the field and the laboratory. *J. Acoust. Soc. Am.* **108**, 2419–2429 (2000).
33. Thompson, L.T. & Best, P.J. Place cells and silent cells in the hippocampus of freely-behaving rats. *J. Neurosci.* **9**, 2382–2390 (1989).
34. Skaggs, W.E., McNaughton, B.L., Wilson, M.A. & Barnes, C.A. Theta phase precession in hippocampal neuronal populations and the compression of temporal sequences. *Hippocampus* **6**, 149–172 (1996).
35. Fyhn, M., Molden, S., Witter, M.P., Moser, E.I. & Moser, M.-B. Spatial representation in the entorhinal cortex. *Science* **305**, 1258–1264 (2004).
36. Jung, M.W., Wiener, S.I. & McNaughton, B.L. Comparison of spatial firing characteristics of units in dorsal and ventral hippocampus of the rat. *J. Neurosci.* **14**, 7347–7356 (1994).
37. Maurer, A.P., VanRhoads, S.R., Sutherland, G.R., Lipa, P. & McNaughton, B.L. Self-motion and the origin of differential spatial scaling along the septo-temporal axis of the hippocampus. *Hippocampus* **15**, 841–852 (2005).
38. Winson, J. Interspecies differences in the occurrence of theta. *Behav. Biol.* **7**, 479–487 (1972).
39. O'Keefe, J. & Recce, M.L. Phase relationship between hippocampal place units and the EEG theta rhythm. *Hippocampus* **3**, 317–330 (1993).
40. Hasselmo, M.E., Bodelón, C. & Wyble, B.P. A proposed function for hippocampal theta rhythm: separate phases of encoding and retrieval enhance reversal of prior learning. *Neural Comput.* **14**, 793–817 (2002).
41. Harris, K.D. *et al.* Spike train dynamics predicts theta-related phase precession in hippocampal pyramidal cells. *Nature* **417**, 738–741 (2002).
42. Bland, B.H. & Oddie, S.D. Theta band oscillation and synchrony in the hippocampal formation and associated structures: the case for its role in sensorimotor integration. *Behav. Brain Res.* **127**, 119–136 (2001).
43. Jensen, O. & Lisman, J.E. Hippocampal sequence-encoding driven by a cortical multi-item working memory buffer. *Trends Neurosci.* **28**, 67–72 (2005).
44. Wallenstein, G.V. & Hasselmo, M.E. GABAergic modulation of hippocampal population activity: sequence learning, place field development, and the phase precession effect. *J. Neurophysiol.* **78**, 393–408 (1997).
45. Ringo, J.L., Sobotka, S., Diltz, M.D. & Bunce, C.M. Eye movements modulate activity in hippocampal, parahippocampal and inferotemporal neurons. *J. Neurophysiol.* **71**, 1285–1288 (1994).
46. Macrides, F., Eichenbaum, H.B. & Forbes, W.B. Temporal relationship between sniffing and the limbic theta rhythm during odor discrimination reversal learning. *J. Neurosci.* **2**, 1705–1717 (1982).
47. Suzuki, W.A. & Clayton, N.S. The hippocampus and memory: a comparative and ethological perspective. *Curr. Opin. Neurobiol.* **10**, 768–773 (2000).
48. Simmons, J.A., Moss, C.F. & Ferragamo, M. Convergence of temporal and spectral information into acoustic images of complex sonar targets perceived by the echolocating bat, *Eptesicus fuscus*. *J. Comp. Physiol. [A]* **166**, 449–470 (1990).
49. Ellins, S.R. & Masterton, F.A. Brightness discrimination thresholds in the bat, *Eptesicus fuscus*. *Brain Behav. Evol.* **9**, 248–263 (1974).
50. Skaggs, W.E., McNaughton, B.L., Wilson, M.A. & Markus, E.J. An information-theoretic approach to deciphering the hippocampal code. in *Advances in Neural Information Processing Systems 5* (eds. Hanson, S.J., Cowan, J.D. & Giles, C.L.) 1030–1037 (Morgan Kaufman, San Mateo, 1993).